Supporting Information

A Long-life Rechargeable Zn Air Battery Based on Binary Metal Carbide Armored by Nitrogen-doped Carbon

Chao Lin,[a] *Xiaopeng Li,**[b] *Sambhaji S. Shinde,*[a] *Dong-Hyung Kim,*[a] *Xiaokai Song,*[c] *Haojie Zhang,*[b] *Jung-Ho Lee**[a]

a Department of Materials and Chemical Engineering, Hanyang University, Ansan, Gyeonggi-do, 15588, Korea. *E-mail: jungho@hanyang.ac.kr

b CAS Key Laboratory of Low-Carbon Conversion Science and Engineering, Shanghai Advanced Research Institute (SARI), Chinese Academy of Sciences (CAS), Shanghai 201210, China. *E-mail: lixp@sari.ac.cn

c School of Chemical & Environmental Engineering, Jiangsu University of Technology, Changzhou 213001, China.

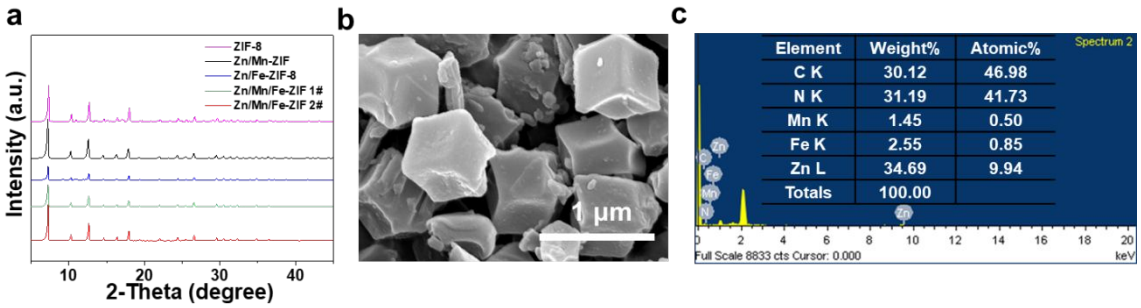

Figure S1. a) XRD patterns of ZIF-8, Zn/Mn-ZIF, Zn/Fe-ZIF, Zn/Mn/Fe-ZIF 1#, and Zn/Mn/Fe-ZIF 2#. b) SEM image of Zn/Fe-ZIF. c) EDS data for Zn/Mn/Fe-ZIF 2#.

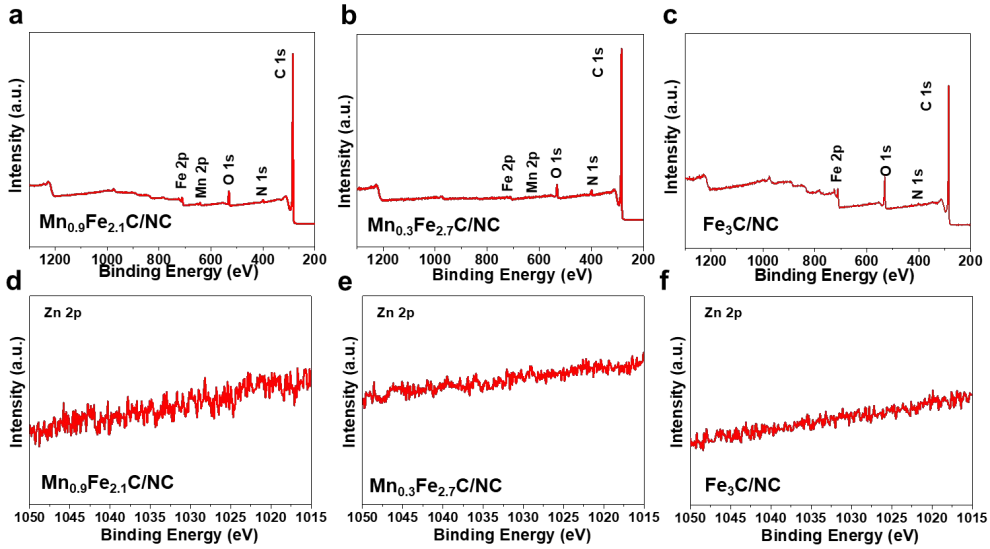

Figure S2. XPS survey and high-resolution spectra for (a, d) $Mn_{0.9}Fe_{2.1}C/NC$, (b, e) $Mn_{0.3}Fe_{2.7}C/NC$, and (c, f) Fe_3C/NC.

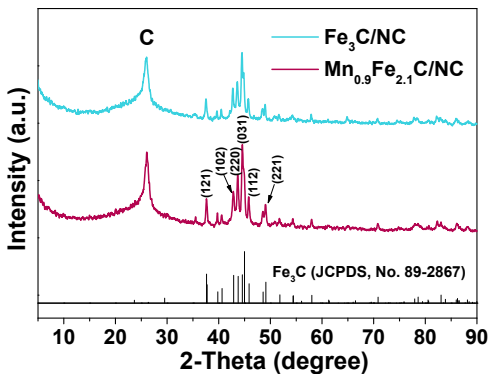

Figure S3. XRD patterns of Fe_3C/NC and $Mn_{0.9}Fe_{2.1}C/NC$.

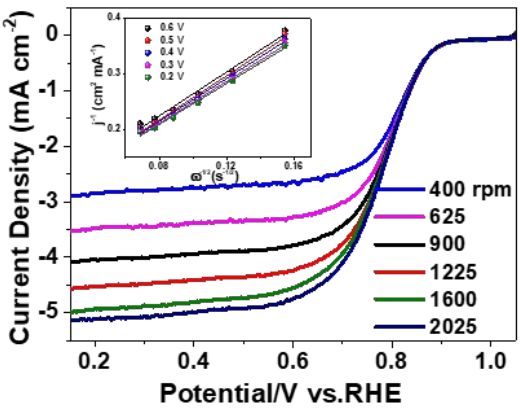

Figure S4. ORR polarization curves of $Mn_xFe_{3-x}C$/NC-2 at different rotation speeds. Inset shows the corresponding Kouteky–Levich plots.

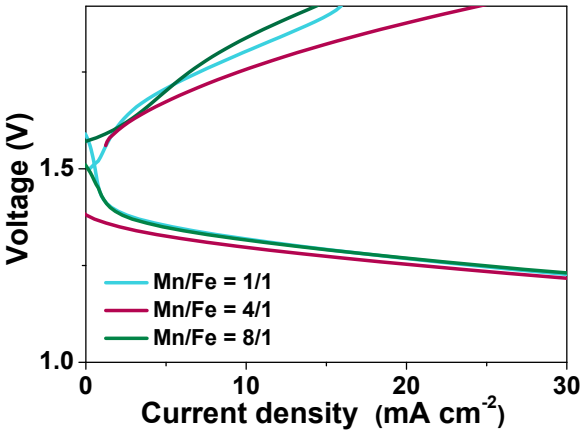

Figure S5. Charge-discharge polarization curves of $Mn_xFe_{3-x}C$/NC catalysts with Mn/Fe precursor ratios of 1/1, 4/1, and 8/1.

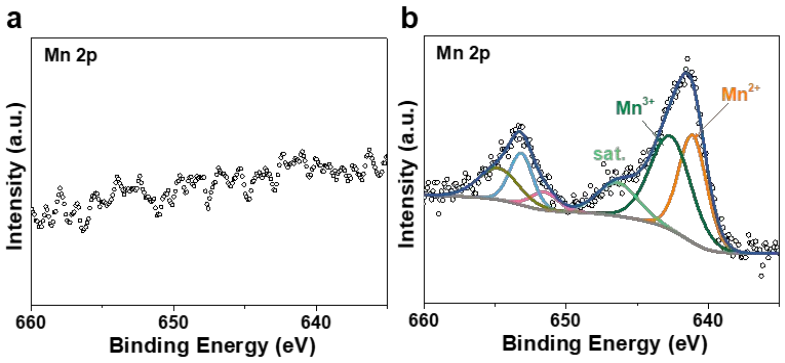

Figure S6. XPS spectra of Mn 2p for (a) Fe_3C/NC and b) $Mn_{0.9}Fe_{2.1}C$/NC.

Table S1. Quantitative XPS analysis results for $Mn_xFe_{3-x}C$/NC and Fe_3C/NC.

	C (at.%)	Fe (at.%)	Mn (at.%)	O (at.%)	N (at.%)
Fe_3C/NC	86.12	2.67	-	9.72	1.49
$Mn_{0.3}Fe_{2.7}$/NC	91.65	0.44	0.05	4.57	3.29
$Fe_{0.9}Mn_{2.1}$/NC	91.52	0.87	0.38	5.17	2.06

Table S2. Atomic concentration of different N species in $Mn_xFe_{3-x}C$/NC and Fe_3C/NC.

	oxidized-N	pyrrolic-N	pyridinic-N	graphitic-N	M-N_x
Fe_3C	0.30	0.38	0.19	0.39	0.23
$Mn_{0.3}Fe_{2.7}$/NC	0.45	0.35	1.06	0.74	0.69
$Mn_{0.9}Fe_{2.1}$/NC	0.42	0.44	0.37	0.39	0.44